

# Contacting single molecules to metallic electrodes by scanning tunnelling microscope manipulation: model systems for molecular electronics

L Grill<sup>1</sup> and F Moresco

Institut für Experimentalphysik, Freie Universität Berlin, Arnimallee 14, 14195 Berlin, Germany

E-mail: [leonhard.grill@physik.fu-berlin.de](mailto:leonhard.grill@physik.fu-berlin.de)

Received 1 December 2005

Published 4 August 2006

Online at [stacks.iop.org/JPhysCM/18/S1887](http://stacks.iop.org/JPhysCM/18/S1887)

## Abstract

The electronic contact between a molecular wire and a metallic electrode will play an important role in future molecular electronics as its properties determine the conductivity of the molecule–metal system. Scanning tunnelling microscopy manipulation reveals various advantages for the investigation of electronic contacts at the atomic scale. In this review, several examples of molecular wire–electrode systems are presented, where single molecules are placed in contact in a controlled way. Changed chemical structures of the molecule and, on the other hand, different shapes and dimensions of electrodes lead to a variety of contact configurations. The contact can be characterized using the additional contribution to the tunnelling current, but also using the influence on the electronic states of the electrode and the molecule. The quality of the contact is discussed in terms of the vertical distance between the molecular wire and the metal atoms and of the chemical composition of the molecular end group.

(Some figures in this article are in colour only in the electronic version)

## 1. Introduction

Remarkable progress has been made in the semiconductor industry in the last few decades as regards the miniaturization of electronic devices. Many technological improvements allowed a decrease of their size, making them smaller and therefore cheaper and faster. These advances follow Moore's law, which states that transistor performance and density double every three years [1]. However, the physical limits of this top-down approach will be reached in the foreseeable future as devices of the size of single atoms or molecules will be required [2]. This makes it important to explore alternatives and conceptually new device structures. A fundamentally new approach is the so-called molecular electronics, the fabrication of circuits

<sup>1</sup> Author to whom any correspondence should be addressed.

at the molecular scale [3–5]. The idea is that single functionalized molecules, i.e. molecular nanomachines, are used as devices that perform the basic functions of digital electronics. The resulting miniaturization is accompanied by advantages offered by the chemical properties of the molecules: self-assembly processes, driven by the intermolecular interactions, can be used to form well-defined structures at the molecular scale [6], while the abilities of synthetic chemistry allow a tailoring of the molecular composition and geometry, thus controlling the molecule's transport, binding, optical and structural properties.

In 1974, Aviram and Ratner had already proposed that a single molecule could act as a rectifier due to its donor–spacer–acceptor structure [7]. Similarly, the chemical structure of more complex molecules can be modified in order to design molecular wires, switches or rectifiers [3]. However, the first experimental studies of functionalized molecules were done more than 20 years later, when the conductivity through single molecules was investigated [8], molecular rectifiers were realized in a multilayer [9] or using single fullerene molecules [10] and the conductance was switched through conformational changes of the molecule [11]. An important class of molecules in this regard are carbon nanotubes with their characteristic physical properties. Experiments have studied their conductivity [12], even over large distances of 1  $\mu\text{m}$  [13], and their ability to be used in a transistor, by switching them from a conducting to an insulating state [14]. The conductivity of different conjugated molecules was determined by connecting them via thiol groups to two colloidal gold particles, which are placed on the electrodes [15]. Another approach for determining the conductivity of a molecule between two electrodes is via the so-called break junctions, where a microfabricated electrode is broken at its centre by mechanical deformation and the resistance of the metallic wire junction is measured. In this way, the conductivity of a very few molecules, which remain in the junction, can be determined directly, the molecules being strongly coupled by thiol groups to gold electrodes [16]. However, its application to single molecules is not straightforward because the conformation, environment and exact number of interconnected molecules remain difficult to determine [17]. Low temperature scanning tunnelling microscopy (LT-STM) is a powerful technique in this regard as it allows one to characterize and image precisely a single molecule–electrode configuration and its surrounding area. Additionally, it offers the possibility of creating a desired geometry by means of manipulation techniques [18].

The basic building units of any circuit in future applications in molecular electronics are the wires, which should enable a controlled maximum charge transport. The conductivities of different systems have been studied theoretically, showing a strong dependence on the chemical structure [19, 20]. However, any functionalized molecular unit in a device must be electrically placed in contact with other units or electrodes. Thus, the electron transport through the contact between the molecule and a metallic electrode plays a crucial role in the quality of a molecular device [21]. It turned out that it is at least as important for the conductivity characteristics of a metal–molecule–metal system as the molecular core [22]. Figure 1 shows a schematic view of such a molecule–electrode junction. A planar geometry of the molecular wire—which must be electronically decoupled from the substrate—is desired, because it facilitates the construction of extended two-dimensional circuits on a surface. The choice of the end groups of the molecule plays an important role when the use of molecular functional units is considered for applications, because they determine the conductance at the molecule–electrode contact (i.e. the contact conductance). A comparison of a benzene and an anthracene group at the end of a molecular wire showed a dramatic difference in contact conductance, with a 20 times larger value for the anthracene group [19].

All results presented are obtained with STM at low temperature, enabling the characterization of molecular wire–electrode systems at the atomic scale, i.e. for single molecules.

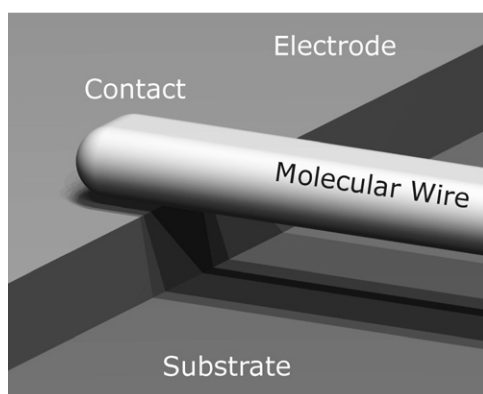
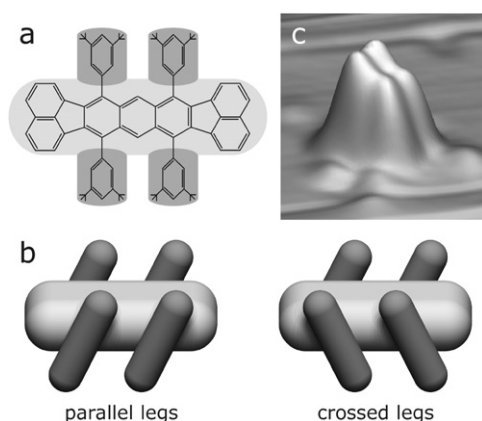


Figure 1. Scheme of a molecular wire–electrode junction.

## 2. Lander molecules

A molecule suitable for placing in contact with a metallic electrode must meet several requirements. First of all, it must consist of a conducting molecular wire (having a small HOMO–LUMO separation), which enables charge transport. When working with metallic substrates, it is necessary to decouple this conducting part electronically from the substrate as otherwise the major part of the charge would flow directly into the metal. One way of solving this problem is by sideways attachment of lateral groups to the molecular wire, which inhibits its direct adsorption on the metal. Additionally, the height of the conducting part of the molecule above the metal must be comparable to the height of monatomic steps on the surface, allowing the creation of a planar contact configuration. All these specifications are met by the so-called Lander molecules (their name originates from the similarity with spacecraft such as the Mars Lander), which have been synthesized by Gourdon [23]. Figure 2(a) shows the chemical structure of the Single Lander molecule, the smallest of the Lander family with a wire length of 1.8 nm. The chemical composition of the polyaromatic central board with two terminal fluoranthene groups for electronic contact, is chosen from a comparison of different types of molecular wires [19]. This central board allows charge transport as it has a band gap of only 1.24 eV [19]. In order to lift the central board up from the substrate, four 3,5-di-*tert*-butylphenyl spacers are attached laterally.

In the gas phase, the lateral legs are approximately perpendicular to the central board [23], while the conditions change upon adsorption on a metal surface. The  $\pi$  system of the polyaromatic board is attracted by the metal substrate and thus the legs are rotated (around their  $\sigma$  bond) off their perpendicular position. Two qualitatively different molecular conformations can be distinguished: the parallel legs and crossed legs conformations (figure 2(b)). In the first case all legs are rotated towards the same side, while in the second one the pairs of legs on each side of the central board are oriented in opposite directions. It is important to note that the legs on the same side of the board must always be parallel due to steric hindrance between the butyl groups. The bulky di-*tert*-butylphenyl groups on the one hand decouple the central molecular wire from the surface and on the other hand dominate the STM images of these molecules. The characteristic appearance of an STM image is shown in figure 2(c), where four bright lobes reflect the four legs of the molecule, while the central board contributes very little to the tunnelling current, according to its decoupling from the surface. Two of the legs appear higher than the other two in a constant current image (i.e. they give a larger contribution



**Figure 2.** (a) Chemical structure of the Single Lander molecule. The central board (light grey) and the four lateral 3,5-di-*tert*-butylphenyl groups (dark grey), acting as legs, are indicated. (b) shows the two conformations of the Lander molecule when adsorbed on a surface: parallel and crossed legs (greyscale tones correspond to (a)). A three-dimensional STM image of a Single Lander molecule on a Cu(110) surface is shown in (c), revealing the different heights of the four lobes.

to the tunnelling current at constant height), even though their topographic height is the same (the molecule is in the parallel legs conformation). This effect is a result of the small distance between two *tert*-butyl groups of neighbour legs as becomes clear from the parallel legs model of figure 2(b). While the right leg offers only one tunnelling channel (through the leg itself), two channels are possible if the tip is positioned above the left leg: one directly through the leg and the other via the overlap of the upper butyl group of the left and the lower butyl group of the right leg, and thus through both legs. Accordingly, the left leg appears higher in the constant current STM images as was found by comparison with molecular mechanics–elastic scattering quantum chemistry (MM–ESQC [24]) calculations [25]. As the orientation of the central molecular wire is deduced from the lateral distances of the legs (larger distance across the board than between neighbour legs), it is possible to determine the conformation of the Lander molecules both from their intensity distribution in STM images and from their shape: square-shaped (parallel legs conformation) or rhombic (crossed legs).

The design of the Lander molecules makes them very attractive when studying molecular wire systems. The smallest exponent of this family, the Single Lander (SL) molecule  $C_{90}H_{98}$  (figure 2(a)), has been studied on various copper surfaces [25–32]. An additional double bond at each end group of the molecular wire leads to the Reactive Lander (RL;  $C_{94}H_{98}$ ) molecule, which has been studied on Cu(110) [33]. In the case of the Violet Lander (VL;  $C_{108}H_{104}$ ), the central part of the molecular wire is elongated, thus increasing the leg separation [34–37]. The largest member of the Lander family is the D-Lander ( $C_{178}H_{190}$ ), having a 3.7 nm long molecular wire and eight legs, i.e. four di-*tert*-butylphenyl groups on each side of the wire [38]. Although the molecular wire is elevated by the spacer groups, it turned out that it is not completely decoupled from the surface. A comparison of several types of Lander molecules, differing in the length of the molecular wire, showed that the scattering pattern of the surface state electrons is dominated by the central board, which thus still interacts with the metal substrate [39].

The adsorption behaviour of Lander molecules on Cu(110) is of particular interest as it leads to the formation of nanostructures of copper atoms. It was first found for Single Landers that the molecules act as templates for the formation of a double row of copper atoms

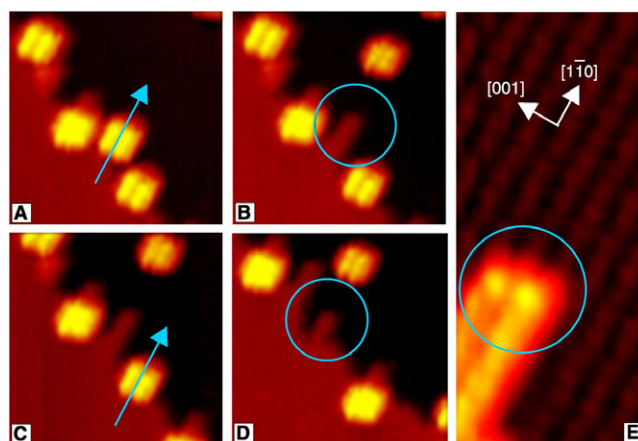


**Figure 3.** ((A)–(D)) Manipulation sequence of Single Lander molecules from a step edge on Cu(110). The arrows mark the molecules that are pushed aside and the circles indicate the nanostructures after removal (all images 13 nm by 13 nm,  $I = -0.47$  nA and  $U = -1.77$  V). The tunnelling parameters for the manipulation are:  $I = -1.05$  nA;  $U = -55$  mV. (E) Smooth-filtered STM image (5.5 nm by 2.5 nm,  $I = -0.75$  nA and  $U = -1.77$  V) of the characteristic copper double row after removal of the Single Lander molecule and the Cu rows of the lower terrace (arrows indicate the surface directions). Reprinted with permission from [27]. Copyright 2002 AAAS.

underneath them [27]. Figure 3 shows the removal of single molecules from the nanostructure with the STM tip. While at these low temperatures (between 100 and 200 K) the structure of the copper double row can be imaged with atomic resolution (figure 3(e)), this is not possible at room temperature as the copper atoms would diffuse as soon as the molecule is removed. The formation of the nanostructure is a thermally activated process (not present at 150 K sample temperature during deposition): the kink copper atoms diffuse along the step edges at room temperature and accumulate under the Lander molecules as soon as they adsorb at a step. Their shape (two atoms wide and seven atoms long) is thus determined by the molecules themselves, which act as templates, while their height is that of the upper substrate terrace. ESQC calculations showed that the central board is lifted up by the nanostructure by more than 1 Å, which reduces the steric constraint on the leg–board  $\sigma$  bonds and leads to a larger distance between two opposite legs in the STM image (compared to adsorption on a terrace) [27].

A detailed study of the molecular conformation on the nanostructure [31] shows that they exhibit parallel and crossed legs conformations, equivalent to adsorption on a terrace. The most common conformation is shown in figure 4(a). As is visible already in the STM image, but more clearly in the line scan across a pair of legs (figure 4(b)), two of the legs (which are closer to the step edge) appear lower than the other two ( $4.2 \pm 0.2$  Å compared to  $4.5 \pm 0.2$  Å). This intensity distribution is in good agreement with the calculated line scan. It shows that—equivalently to adsorption on a terrace (see above)—the molecule is in the parallel legs conformation, having all legs rotated towards the upper terrace. This is the lowest energy conformation, and therefore the most frequent after adsorption, as has been shown by total energy calculations.

The deposition of Reactive Lander, instead of Single Lander, molecules onto Cu(110) shows exactly the same phenomenon, leaving copper nanostructures after removal of the molecules [33]. The dimensions of the copper ‘tooth’ are equivalent (two by seven atoms), according to the almost identical chemical composition. When depositing the Violet Lander molecules, the resulting nanostructures are nine atoms long due to the longer central board of

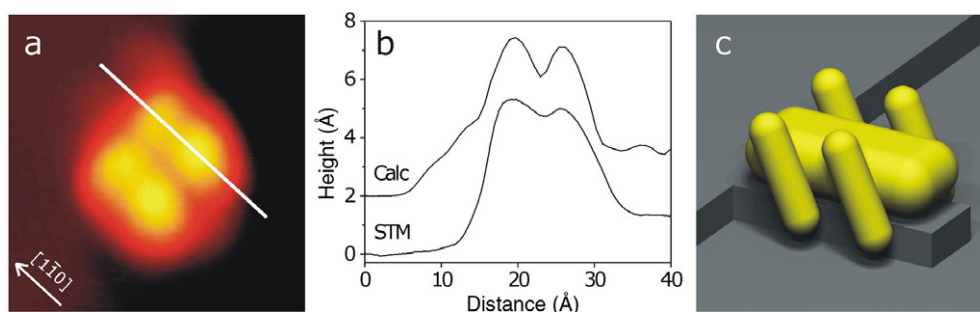


**Figure 4.** Determination of the molecular conformation of a Single Lander molecule adsorbed on a nanostructure on Cu(110) [31]. (a) shows an STM image ( $40 \times 40 \text{ \AA}$ ,  $I = 0.2 \text{ nA}$  and  $U = 1.5 \text{ V}$ ) of a single molecule (upper terrace at the left, lower terrace at the right). (b) A comparison of a calculated (calc) and an experimental (STM) line scan across a pair of legs in the  $[1\bar{1}0]$  direction (the experimental line scan is marked in (a)). (c) A model of the parallel legs conformation of the molecule.

the molecule [36]. Although the width of most nanostructures is still two atoms, a minor part with a triple row of copper atoms is found, reflecting the modified chemical structure of the molecular wire (the lateral distance of opposite legs is the same as for SL and RL).

### 3. Creating a contact configuration

When organic molecules are deposited onto single-crystal surfaces, the kind of growth mode is determined by the balance between the deposition and the diffusion rate, which depends on the substrate temperature [6]. When adsorption takes place at low temperatures, molecular diffusion is inhibited and the hit-and-stick adsorption mode leads to a random distribution of molecules. The molecules adsorb at minima of the potential landscape, i.e. energetically preferred sites like defects and step edges. However, all these adsorption geometries of molecules are unlikely to reflect the desired geometry of an electronic contact with a metallic electrode as shown in figure 1, as this is obviously not the lowest energy configuration of a molecular wire. The use of molecules equipped with spacer legs is advantageous, because the legs elevate the wire from the substrate. Adsorption of such Single Lander molecules and subsequent annealing leads to their adsorption at step edges. However, they do not adsorb in a contact geometry having only the end of the molecular wire in contact with the step edge (as interpreted previously [26]), but with two legs on the upper and two on the lower terrace. It is therefore necessary to use STM manipulation techniques in order to obtain the molecular conformation and adsorption site that is desired by means of an electronic contact.

The manipulation of an atom or a molecule with the STM tip is based on the interatomic forces between the metallic tip and the atom/molecule [18, 40]. Uncontrolled diffusion of the adsorbate must be inhibited during the experiment; therefore cryogenic temperatures are required. In the experiment, the tip is usually moved laterally across the adsorbate using parameters that provide forces sufficiently large to overcome the diffusion barrier. Depending on the driving force of the process, single atoms and molecules can be moved laterally on a surface either in a ‘pushing’ (repulsive forces) or in a ‘pulling’ (attractive forces) mode [41, 42]. Three parameters are varied in the experiment to control the manipulation process: the tip height, the pathway of the tip during manipulation and the applied bias voltage (resulting in a characteristic tunnelling current and electric field in the junction). By using suitable parameters, nanostructures are built from single atoms [43] or molecules [44] by precise positioning at

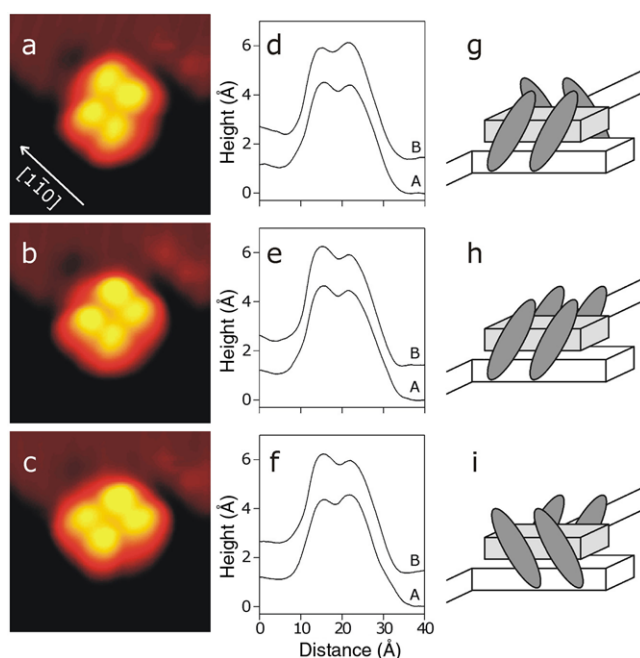


**Figure 5.** Intramolecular manipulation of a Single Lander molecule adsorbed on a copper nanostructure on Cu(110). The central board does not move during manipulation. ((a)–(c)) STM images ( $45 \times 45 \text{ \AA}$ ) of different conformations. The corresponding line scans across the legs in the  $[1\bar{1}0]$  direction are plotted in (d)–(f) (line scans A across the ‘lower’ pairs of legs and B, shifted vertically by  $1.5 \text{ \AA}$  for clarity, across the ‘upper’ ones in the STM images). (g)–(i) show schematic models of the molecular conformations. Reprinted with permission from [31]. Copyright 2004 by the American Physical Society.

chosen adsorption sites. An increase of the molecular size is typically accompanied by a rise of the diffusion barrier [45], which requires larger forces applied by the tip and holds the risk of dissociation. The complexity of the molecule thus determines the limit of lateral molecular manipulation (as shown for molecular wheelbarrows [46]), because an increase in the molecular functionalities leads to larger molecules. Apart from lateral translation of a molecule, the intramolecular conformation of a molecule can also be modified by manipulation in a controlled way. It has been shown that the orientation of a lateral leg of a single Cu-tetra-3,5 di-*tert*-butylphenyl molecule can be changed reversibly by vertical or lateral motion of the STM tip, realizing the principle of a conformational molecular switch [47].

The challenge in the creation of a contact configuration by means of STM manipulation is twofold: first the molecule must be laterally manipulated to an adsorption site suitable for a contact, and second the intramolecular conformation must be controlled for a precise contact configuration. The latter point concerns in particular the position of the lateral legs of a Lander molecule (figure 2), avoiding lateral translation of the entire molecule. An interesting system in this regard is the Lander molecule adsorbed on a copper nanostructure (figure 4). As the molecular board is lifted up by the nanostructure, it is possible to rotate by lateral manipulation only a single pair of legs, leaving the opposite legs and the central board unchanged [31]. In this way, the molecule can be reversibly switched between different parallel and crossed legs conformations as presented in figure 5. The conformations are identified from comparison with ESQC calculations and from the characteristic intensity distributions of the molecular legs,

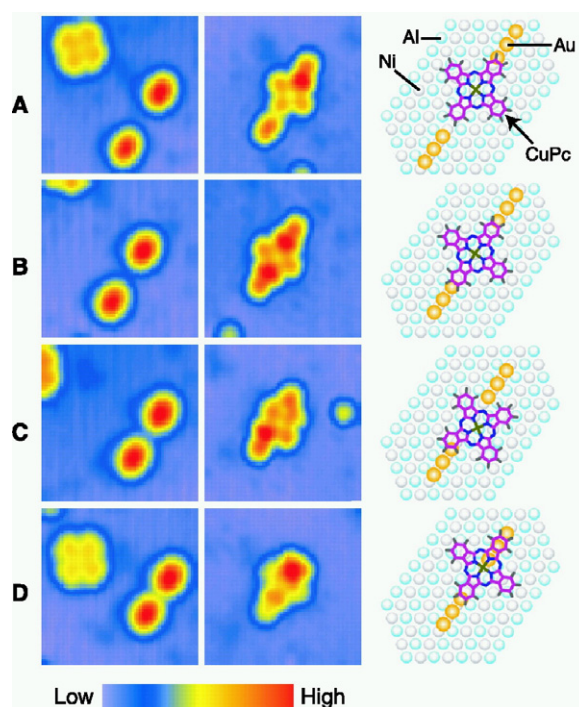


**Figure 6.** Cu(II) phthalocyanine (CuPc) molecules placed in contact with Au chains on NiAl(110). Left column: bare  $2\text{Au}_3$  junctions before the molecules were added (imaging conditions:  $U = 1\text{ V}$ ,  $I = 1\text{ nA}$ ; the image size is  $47\text{ \AA}$  by  $47\text{ \AA}$ ). Middle column: assembled hybrid structures ( $U = 0.5\text{ V}$ ,  $I = 1\text{ nA}$ ; these imaging conditions emphasize the molecular adsorption configuration). Right column: the scheme attributed to each adsorption configuration. (A) Six Ni–Ni lattice constants between the  $\text{Au}_3$  chains. (B) Five lattice constants. (C) Four lattice constants. (D) Three lattice constants. Reprinted with permission from [49]. Copyright 2003 AAAS.

obtained from the line scans in (d)–(f). Note that no motion of the entire molecule occurs, as becomes clear from the fixed defects in the upper right in the STM images.

### 3.1. CuPc molecules on Au nanostructures

A simple system that realizes approximately the placing of a molecule in contact with a metallic electrode is the partial positioning of a molecular wire on an atomic-scale nanostructure. It has been shown that such a system can be achieved by placing a pentacene partially on an assembled Cu chain, resulting in an electronic interaction between the molecule and the copper atoms [48]. However, such a system does not satisfy the conditions for a contact configuration (figure 1), because the molecular wire is neither planar nor decoupled from the substrate.

A more advanced system is the Cu(II) phthalocyanine (CuPc) molecules, which are manipulated onto assembled gold electrodes on a NiAl(110) substrate [49]. In a first step, short chains of gold atoms, lying in a row, are assembled on a NiAl(110) surface by STM manipulation. On positioning the molecule between two Au chains, it bridges the gap between the electrodes in a planar configuration. Figure 6 shows this step of the contact creation for different distances between two  $\text{Au}_3$  chains. The left column shows STM images before the molecular manipulation, having the CuPc molecule (which appears as a square of four lobes) still lying flat on the terrace. The molecules were then moved into the junction between the two

electrodes, where they are found to be more stable than on the terrace. The middle column of figure 6 shows the corresponding STM images for different distances between the two electrodes. It turns out that for the case of a gap of six lattice constants (A) the molecule is placed in contact with the upper electrode, but not the lower one, as the gap is too large. Having a gap between the electrodes of four or less lattice constants, the molecule is distorted out of a symmetric adsorption configuration (figures 6(C) and (D)). The best environment is found when a gap of five lattice constants is used (B): the molecule adsorbs symmetrically with two opposite benzene rings attached to the two gold electrodes. In this optimal geometry, equivalent lobes, which are caused by the electronic interaction between the molecule and the electrode, are visible at the two contact positions. This configuration matches quite well the contact geometry presented in figure 1 in terms of a planar molecule that has its end group in contact with an electrode (in the present case even placed in contact with two electrodes). Moreover, it allows complete access to the entire molecule with the STM tip. However, it cannot be considered as a model system for a contact configuration by means of electron transport measurements, because the molecule is not decoupled from the conducting substrate and the gold clusters are too small to develop metallic character [49].

### 3.2. Single Lander molecules on Cu(111)

A type of molecule which has been especially designed for placing in contact with an atomic-scale electrode is the Lander molecule (see section 2). The spacer legs lift the central molecular wire up in order to decouple it from the substrate. The resulting height of the central board is between 3 and 4 Å on a low index single-crystal copper surface [25, 30, 33], and thus of the order of a monatomic step height. This characteristic has been used to place a Single Lander molecule in contact with a step edge of the Cu(111) surface [30] as shown in figure 7. A molecule adsorbed on the terrace (column A) shows the characteristic intensity distribution of the parallel legs conformation, identified by the ESQC calculation technique (figure 7(A2)). It acts as a scattering centre for the two-dimensional electronic surface states and creates an almost circular standing wave pattern [39] around each molecule (figure 7(A4)).

In order to place the Single Lander in contact with a monatomic step, a chosen molecule is laterally manipulated with the STM tip in constant height mode [50]. As the orientation of the central molecular wire is known from the appearance, the molecule can be positioned at the step edge either parallel or perpendicular to it. The first case is shown in column B of figure 7. In this parallel orientation the final configuration is given by the van der Waals distance of the lower CH<sub>3</sub> groups of the legs from the step edge, i.e. the molecule is as close as possible to the step edge. In this geometry, obviously no interaction of the molecular wire with the step edge is observed. However, a clear modification of the standing wave patterns is visible if the central molecular wire is oriented perpendicular to the step edge (figure 7(C4)). The molecule is found in the STM image to be in contact with the step edge, with the terminal naphthalene group of the wire on top of the step edge (extracted from ESQC calculations). As a result, an increased apparent height, a so-called contact bump (see section 4.3), appears in the STM image at the position of the naphthalene group. It is important for the observation of the electronic contact that the molecule is in the parallel legs conformation with all legs rotated towards the lower terrace. Any other crossed or parallel legs conformation reduces the access of the STM tip to the contact point and therefore attenuates the visibility of the contact bump.

Note that the step edge in the manipulation series of figure 7 is perfectly straight. This condition is important for the precise placing in contact with a molecular wire, because the atomic structure of the electrode must be well defined. In the experiment, the quality of these step edges would not be offered by intrinsic steps, which exhibit kink atoms and are often

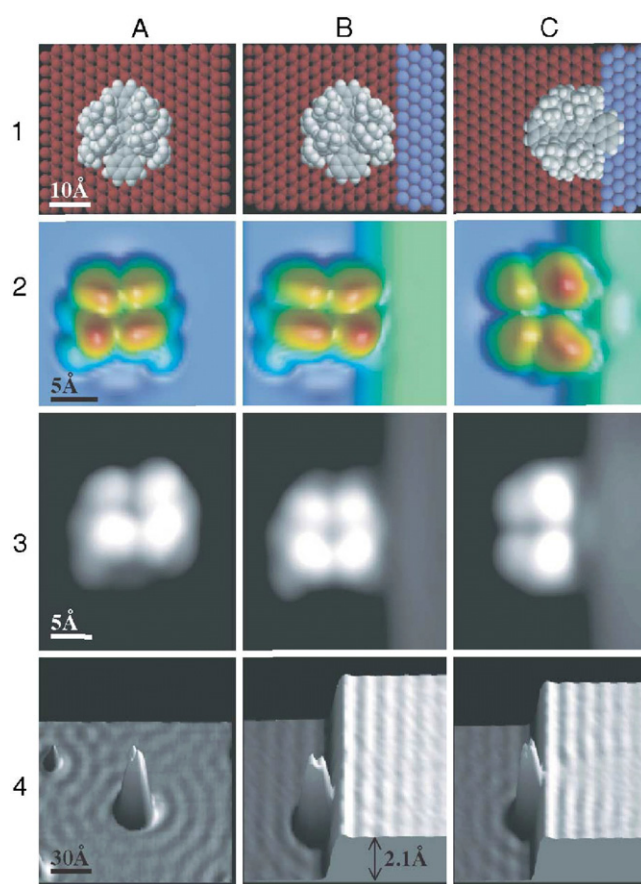


**Figure 7.** Single Lander molecules on a Cu(111) terrace (col. (A)) and placed in contact with a (100) step of an edge dislocation. The molecule can be positioned with the molecular board parallel (col. (B)) or perpendicular (col. (C)) to the step. Only in the latter case an influence, due to the molecular board, on the upper terrace become visible. In (2C) and (3C) an additional bump corresponding to the point of contact of the wire with the step appears and in (4C) a modification of the upper terrace standing wave patterns is visible. Row 1: sphere models of optimized molecular structures. Row 2: calculated STM images, corresponding to the models above. Row 3: STM measurements. Black to white distance 3.5 Å,  $U = 0.8$  V,  $I = 0.2$  nA,  $T = 8$  K. Row 4: three-dimensional STM images visualizing the standing wave patterns ( $U = -0.1$  V,  $I = 0.2$  nA,  $T = 8$  K). Reprinted with permission from [30]. Copyright 2003 by the American Physical Society.

covered with slight contamination of the deposition procedure. The step edges for the contact experiments are created by a controlled crash of the tip into the surface, thus forming glide plane dislocations several hundred nm long with monatomic height [30]. After the step formation, the tip is moved laterally away from the crash zone to find an atomically clean surface area with the presence of dislocation steps.

### 3.3. Single Lander molecules on Cu(110) nanostructures

The use of electronic contacts for devices requires miniaturized electrodes rather than laterally extended step edges as presented in section 3.2 (or in the scheme of figure 1). Ideally, these

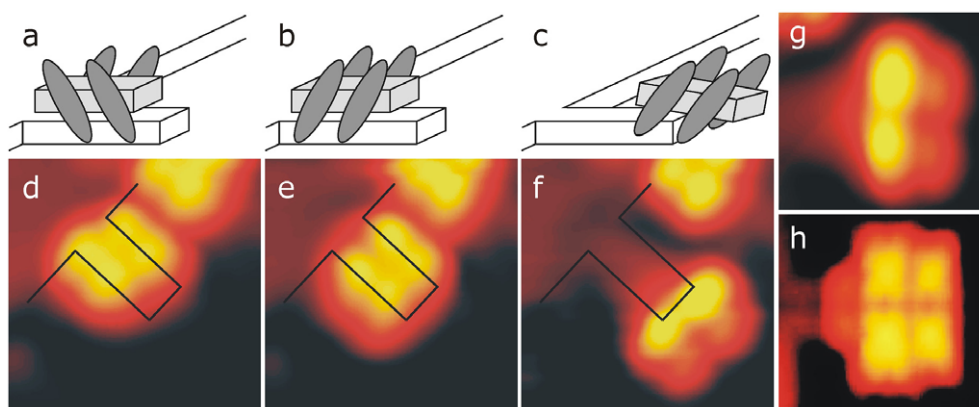


**Figure 8.** Lateral manipulation of a Single Lander molecule along a Cu(110) nanostructure. ((a)–(c)) Schematic models and ((d)–(f)) corresponding STM images ( $45 \text{ \AA} \times 45 \text{ \AA}$ ) during the lateral manipulation along a tooth. The black lines, drawn to point out the different molecular positions, mark the step edge and the position of the Cu nanostructure ( $8.0 \pm 0.2 \text{ \AA}$  wide and  $17.7 \pm 0.4 \text{ \AA}$  long) under the Lander as determined from an STM image after the removal of the molecule. (g) STM image of the final position with a tilted molecular board (equivalent to (f)) and (h) corresponding calculated image (both  $25 \text{ \AA} \times 23 \text{ \AA}$ ). Reprinted with permission from [31]. Copyright 2004 by the American Physical Society.

electrodes should act as contact pads for a molecular wire with suitable dimensions, thus having a width comparable to the width of the wire. Nanostructures of this type can be fabricated precisely at the atomic scale by manipulation with the STM tip, which was shown for Au chains one atom wide on NiAl(110) (section 3.1). However, this is not a useful approach for the fabrication of electronic circuits, where many pads of well-defined dimensions are needed. The Lander molecules exhibit an interesting adsorption behaviour when deposited at room temperature onto Cu(110), because they act as templates for the formation of characteristic nanostructures under them (figure 3) [27]. As the dimensions of the nanostructure (two atoms wide and seven atoms long for a Single Lander) are determined by the molecular size, it fits very well with the width of the central molecular board. The nanostructure, which always extends from a step edge, is therefore very suitable for acting as a contact pad for the Lander molecules.

In order to create a contact configuration, the molecules, which adsorb on the nanostructure directly after deposition (figure 4), must be moved very carefully towards the lower terrace in order to have only one end of the central wire in contact with the pad. While a complete removal requires the application of forces for a sufficiently large pathway, it is more difficult to move the molecule in very small steps of the order of substrate lattice constants. Figure 8 shows a manipulation series for a single SL molecule on a nanostructure. The manipulation procedure is done at a tunnelling resistance of about  $50 \text{ k}\Omega$  while  $100 \text{ k}\Omega$ , i.e. a larger tip height, is used for the controlled change of the molecular conformation (figure 5). This reflects that, having the same tip pathway during manipulation, the forces necessary for a motion of the entire molecule are larger than for a conformational change. In this way, the molecule is moved in small steps along the copper wire and adapts to different positions (figures 8(d)–(f)) before it is pushed away from the nanostructure.

The first position in figure 8(d) is the initial one directly after deposition. In contrast to being in the common configuration, in which the vast majority of molecules adsorb in a parallel conformation (figure 4), the imaged Lander is here in a crossed legs conformation, reflected

by the rhombic shape. Only about 10% of the Landers adsorb directly in this conformation, which can also be achieved artificially by lateral manipulation (figure 5). After the first lateral manipulation, the molecular board is still planar, but shifted by a few ångströms with respect to the initial position (figure 8(e)). In addition to the translation of the molecule, the conformation changed from crossed to parallel legs. This configuration is never found after deposition, because the energetically preferred site is the one next to the step edge. However, this is still not a suitable contact conformation, because the entire molecular wire is adsorbed on the nanostructure.

In figure 8(f) the molecule has reached the end of the wire and is adsorbed in the so-called tilted board conformation, which was predicted by total energy calculations [31]. The appearance of this conformation (g) is in good agreement with the calculated image (h): the two lobes close to the Cu wire appear much brighter in the STM image than the other ones, showing that the molecular board is tilted with respect to the flat conformations on the nanostructure or on the terrace, while all legs are rotated towards the lower terrace. Any further tip-induced shift results in a complete removal from the nanostructure leaving the molecule on the lower terrace. This tilted board conformation reflects quite well the contact configuration of a molecular wire, as the end group is in contact with an atomic-scale electrode that has about the same width as the molecular wire. Although the central board is not in a planar configuration, it is elevated from the substrate by the spacer legs.

#### 4. Characterization of the electronic contact

When the interatomic distance between the STM tip and a molecule is decreased, the so-called mechanical contact occurs at rather large distances, where the van der Waals and repulsive forces are balanced in the junction, giving rise to a deviation in the current signal as a function of the tip height. The electronic contact between a molecule and a metallic electrode is reached later at the beginning of molecular orbital mixing, which has been studied for the contact between an STM tip and a single  $C_{60}$  molecule [51]. The contact of a molecular wire with an metallic electrode is therefore expected to affect both the molecular orbitals and the electronic states of the electrode. Additionally, the tunnelling current, which passes through the contact between the STM tip and sample, at this position increases, leading to the so-called ‘contact bump’ (or larger apparent height, if the measurements are done in the constant current mode). These different consequences of a molecule–electrode contact are discussed in the following.

##### 4.1. Modification of the local electronic structure

The electronic properties of the molecular wire and the electrode can be measured by scanning tunnelling spectroscopy (STS). By using the lock-in technique, differential conductance spectra  $dI/dV$ , which are a measure of the local density of states (DOS), are determined with high spatial resolution. It is therefore a useful technique for studying the changes in the electronic structure in the environment of an electronic contact. Figure 9 shows the  $dI/dV$  spectra at different characteristic points close to the contact in the case of the CuPc molecule placed in contact with two opposite gold chains (see section 3.1). The length of the gold chains is changed in this series, starting from the bare CuPc molecule in A to two chains of six atoms length in G. The right panel in figure 9 shows the  $dI/dV$  curves of the unoccupied electronic states: (a)–(c) correspond to the local DOS of the molecule, while the electronic structures of the gold chain with and without the molecule are plotted in (d) and (e), respectively.

As can be clearly seen, the placing in contact with the molecule leads to a downshift of the molecular orbitals ((b) in figures 9(A) and (B–G), respectively). This effect has already

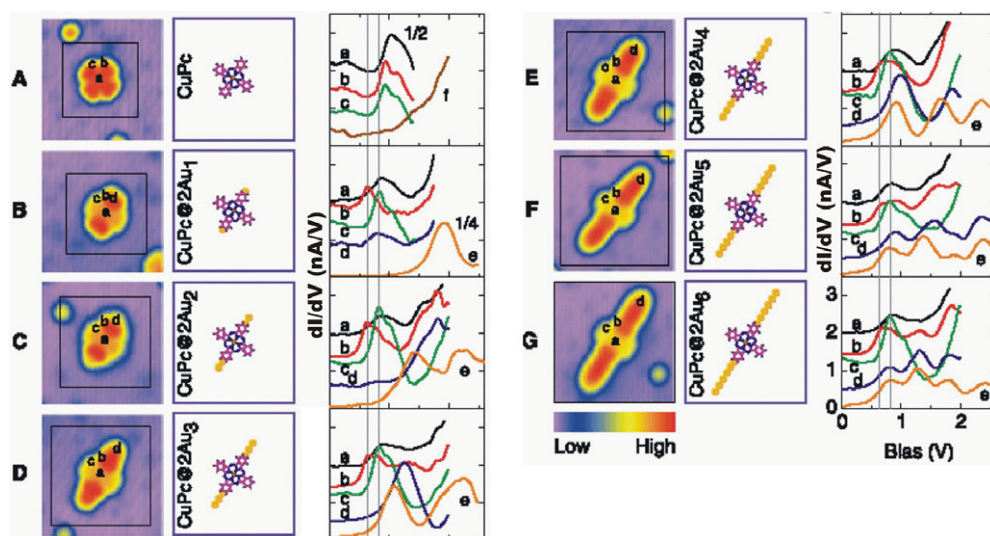


**Figure 9.** Left column: topographies for different  $\text{CuPc}@2\text{Au}_n$  structures, from (A) an isolated  $\text{CuPc}$  molecule on  $\text{NiAl}$  ( $n = 0$ ) to (G)  $\text{CuPc}@2\text{Au}_6$  ( $\text{CuPc}$  on two  $\text{Au}$  chains containing six atoms each); all STM images:  $47 \text{ \AA}$  by  $47 \text{ \AA}$ ,  $U = 1 \text{ V}$ ,  $I = 1 \text{ nA}$ ,  $T = 13 \text{ K}$ . Data were obtained in different experimental runs, causing slightly different orientations of the sample, as can be seen in (F). Middle column: schematic diagrams of the corresponding  $\text{CuPc}@2\text{Au}_n$  structures. Right column:  $dI/dV$  spectra taken at key locations on the  $\text{CuPc}@2\text{Au}_n$  structures are given by curves (a), (b), (c), and (d); spectra for bare  $\text{Au}_n$  chains and  $\text{NiAl}$  are given by curves (e) and (f), respectively. The exact locations where the spectra were measured are noted in each topography image. For all of the structures except the free molecule, spectra were measured with set-point  $U = 1.75 \text{ V}$ ,  $I = 1 \text{ nA}$ . Spectra for the free molecule (adsorbed on  $\text{NiAl}$ ) were taken with set-point  $U = 1 \text{ V}$ ,  $I = 1 \text{ nA}$ , and scaled by a factor of 0.5. The bias range for free molecule spectra was reduced to avoid molecular motions that could be induced at  $U > 1.4 \text{ V}$ . Upon adsorption on the  $\text{Au}$  chains, the molecules became more stable, which allowed the extension of the scan range to higher voltages. Curve (e) in (B) was scaled by a factor of 0.25. The two vertical lines at 0.63 and 0.82 V show the positions of molecular peaks in curves (b) and (c). Reprinted with permission from [49]. Copyright 2003 AAAS.

arisen upon the placing in contact with a very short ‘chain’ of one atom, while no clear further energetic shift is observed when more gold atoms are added to the electrode (figures 9(C)–(G)). The molecular orbitals are therefore almost completely determined by the interaction with one gold atom, even if the electrodes consist of more than one. The interaction with one single atom is thus sufficient for creating an electronic contact of a molecule. A detailed analysis of the molecular orbitals shows that the distance to the gold atoms changes the energetic shift: the orbital at 0.63 eV exhibits a larger downshift in energy than the 0.82 eV orbital, due to its closer proximity to the gold atoms [49].

At the same time, the electronic structure of the gold chain is changed by the interaction with the molecule: the peaks in the spectra (d) are shifted to higher energies with respect to the peaks of the isolated chains. This effect is due to the modification of the gold electronic state which is in direct contact with the molecule and therefore shifted out of resonance [49]. In contrast to the molecular orbitals, the electronic states of the  $\text{Au}$  nanostructure shift upon extension of the chain (curve (d) in (B)–(G)), even without a molecule in contact (e). This is due to the quantum well character of the one-dimensional gold chain and the resulting electron confinement [52]. However, the relative energetic shift caused by the placing in contact with the molecule is about the same for chain lengths up to five atoms and thus already determined when

the molecule is in interaction with a single atom. Note that, if the gold chain is six atoms long, almost no difference is found between the electronic structures with and without a molecule placed in contact at the free end of the nanostructure.

These results show that the electronic structures of both the molecular system and the metallic electrode are very sensitive to the interaction in a contact junction and are therefore useful fingerprints for the characterization of an electronic contact. The  $dI/dV$  curves reveal that the contact of the molecule with one single gold atom already determines the energetic shift of the electronic states and the molecular orbitals, as it does not change significantly upon further elongation of the nanostructure (two and more atoms). This situation is comparable to the case of an 'extended molecule', where thiol-substituted molecules strongly attract gold atoms of an electrode and the gold atoms, which are in direct contact with the molecule, can therefore be considered part of the 'extended molecule' [53].

#### 4.2. Scattering of surface state electrons

Defects on a metal surface, which exhibits a Shockley-type surface state, cause the scattering of surface state electrons [54]. The resulting standing wave patterns in the local density of states can be observed by STM at low bias voltages. By scanning an STM image in the differential conductance mode, so-called  $dI/dV$  maps at a certain bias voltage are obtained, revealing spatial information on the electronic DOS. In this way, the standing wave patterns can be studied as a function of the energy. The shape of the standing waves depends on the electron energy (the wavelength decreases with increasing energy, according to the parabolic dispersion relation) and in particular on the geometry of the scatterer [55]. By using a complex system as an organic molecule as scatterer, it is possible to relate the internal structure of the molecule to its standing wave pattern [39]. It was shown that the relative weight of each scattering centre in the molecule accurately determines the standing wave pattern, which is thus a fingerprint of the interaction of the molecule with the substrate.

This means for an electronic contact that the standing wave pattern on the electrode surface could be used as a feature for the characterization. Two conditions must be met for such a system: first, the electrode must exhibit a suitable surface state, like Cu(111) or other noble metal (111) surfaces. Second, the proportions of the electrode must be suitable for the characterization of the standing wave pattern. This concerns on the one hand the size, which must be of the order of at least several wavelengths, and on the other hand the border (step edge) of the electrode, which acts as a scatterer and therefore determines the pattern on the bare electrode. This pattern must be well defined for investigating the changes induced by the molecule placed in contact, requiring atomically straight electrode borders. The Lander/Cu(111) system (section 3.2) meets all these requirements, because the electrode is an extended Cu(111) terrace with a sharp and well-defined edge, which is a perfectly straight dislocation step (created artificially by a controlled tip crash).

Figure 10(A) shows the experimentally determined standing wave pattern on the upper terrace, when a Single Lander molecule is placed in contact with the step edge (see figure 7(C)). It can be clearly seen how the parallel electron density pattern is attenuated in the vicinity of the Lander contact position. This STM image is compared in B to a calculated one, based on the scattering formalism of Heller *et al* [55]. Figure 10(D) shows the arrangement of the scatterers: a line of equally spaced black dots with a nearest neighbour distance of 2.55 Å, representing the step edge, and four black dots, displaced by 2.8 Å perpendicularly off the line, representing the contact. These values lead to the calculated standing wave pattern presented in B which is in very good agreement with the experimental data: both show the perturbed area of approximately triangular shape descending from the contact point. The line

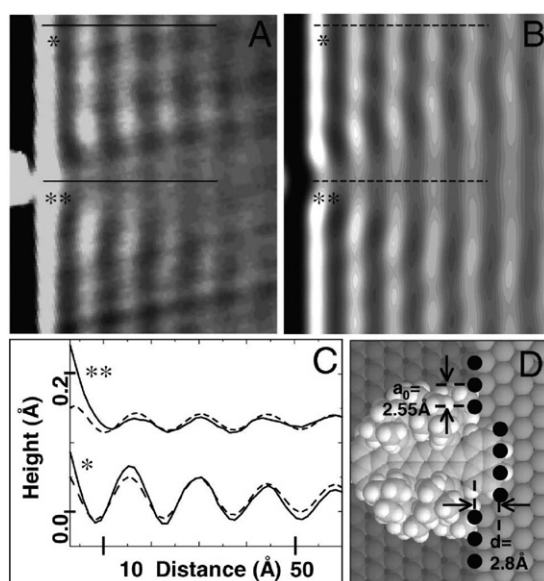


**Figure 10.** Electron density patterns in the vicinity of a Single Lander molecule placed in contact with a Cu(111) step edge. (A) Measured image ( $9 \times 11$  nm;  $U = -0.1$  V,  $I = 0.2$  nA,  $T = 8$  K). (B) Calculated electron density pattern for a scattering geometry as sketched in D (image size:  $9 \times 11$  nm), height in arbitrary units. (C) Line scans, taken from the measurement (solid lines) and calculation (dashed lines). The line scans are taken at the positions indicated in (A) and (B). The height scale of the calculation has been adjusted to match the experiment. (D) Model of the geometry of scatterers (black dots) used for the calculation; the model derived by the molecular mechanics calculation is shown faintly in the background for comparison. Reprinted with permission from [30]. Copyright 2003 by the American Physical Society.

scans in figure 10(C) emphasize this similarity for the height profiles at the contact point (upper curves) and several nm off (lower curves). As presented in D, the size and position of the black dots reflect very well the dimensions and position of the molecular board, as determined by molecular mechanics calculations. This shows that the modification of the standing wave pattern on the upper terrace is caused by the naphthalene end group of the molecular wire, which interacts via coupling of the  $\pi$  molecular orbitals with the upper terrace surface states. Thus, the electronic contact of the molecular wire with the Cu(111) step electrode is characterized in this way using the influence of the electron standing waves of the metal electrode.

#### 4.3. 'Contact bump'

The electronic contact of a molecule with an electrode leads to an increased apparent height in the STM image (taken in the constant current mode; the tunnelling current is increased if scanning is done at constant tip height), called a contact bump in the following, which is observed in the experiments presented above (figures 6–8). It is the remaining part of the STM contrast that the molecular wire would provide if adsorbed alone (without the legs in the case of a Lander molecule) on the surface in the same adsorption geometry [31]. This change in the STM contrast measured at the contact position can be used as a measure of the metal–molecular wire–metal junction contact conductance [56]. Thus, the intensity of the contact bump, obtained from experimental height profiles, can be used for a quantitative description of

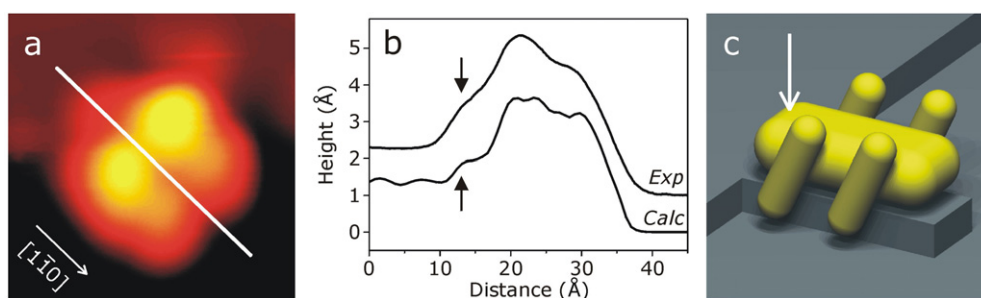


**Figure 11.** Determination of the ‘contact bump’ from an STM image [33]. (a) shows a Reactive Lander molecule adsorbed on a copper nanostructure ( $35 \times 35 \text{ \AA}$ ,  $I = 0.3 \text{ nA}$ ,  $U = 0.5 \text{ V}$ ) in the parallel legs conformation with all four legs rotated towards the lower terrace as shown in the schematic view (c). An experimental line scan, taken in the  $[1\bar{1}0]$  direction across the central board of the molecule (as indicated in the image), is compared in (b) with a calculated one (identified as *exp* and *calc*, respectively). The arrows mark the position of the ‘contact bump’, visible as a shoulder in the height profile. The position of this bump is marked in the scheme (c) by an arrow.

the electronic interaction. Figure 11 shows how the increase of the STM apparent height  $\Delta h$  at the end board location is extracted from line scans across the centre of the molecule. In this case of a Reactive Lander, the spacer legs of the molecule are much higher than the molecular wire and dominate the STM image. The contact bump thus appears as a shoulder (marked by an arrow in (b)) in the intense contribution from the molecular legs. Note that the calculated line scan exhibits a smaller contribution from the legs, as the real tip apex is presumably broader than the one assumed in the calculations. The lateral position of the contact bump is in accordance with the calculation and can therefore be assigned to the end group of the central molecular wire (indicated in (c)). To obtain quantitative information from the contact bump, a background caused by the molecular legs is subtracted, in order to consider exclusively the contrast due to the end part of the board. The resulting  $\Delta h$  amplitude can be used as a measure of the electronic interaction between the contact molecular wire and the metallic electrode. This is in particular important for the relative changes in a comparison between similar contact configurations where e.g. the interatomic distance between the molecule and the electrode or the chemistry of the wire end group is changed (see below).

## 5. Dependence on the electrode–molecule distance

The characteristics and quality of a contact for quantum transport depend on the electronic interaction between the molecular wire and the metal atoms. An important parameter in this regard is the interatomic distance between the molecular wire and the metallic electrode as it determines the orbital mixing. The lateral position with respect to the electrode is of minor importance in this context, because it modifies primarily the fraction of the wire that is placed in contact. It is the vertical distance that mainly defines the interaction, i.e. the molecular wire needs to be moved up and down while the planar geometry of the wire should ideally be maintained (see figure 1). While the vertical position of a molecular wire can be chosen in model calculations, it is a challenge to perform an equivalent experiment. After physisorption or chemisorption on the terrace of a metal, the chemical properties of a molecule define its adsorption distance from the substrate atoms [57]. Even though various adsorption sites or orientations of the molecule might be present, the vertical distance above the surface does not vary strongly. It is therefore necessary to study a molecule which adapts

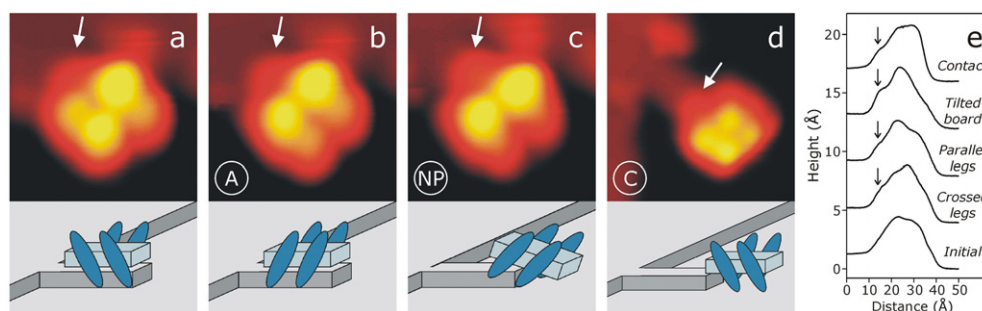


**Figure 12.** STM images and corresponding schemes (upper and lower panel respectively) of different conformations of the Reactive Lander molecule on the Cu(110) nanostructure, achieved by lateral manipulation with the STM: (a) crossed legs conformation, (b) parallel legs conformation (called A), (c) tilted board conformation (NP) and (d) contact conformation (C). STM images are  $35 \times 35 \text{ \AA}$  ((a)–(c)) and  $45 \times 45 \text{ \AA}$  (d) in size. The arrows mark the location of the contact bump, reflecting electronic interaction between the molecular wire and the nanostructure (see text). (e) Height profiles across the central molecular board along the substrate direction  $[1\bar{1}0]$  for all conformations of the RL molecule (the upper terrace is on the left side in all height profiles). The arrows mark the contact bump with the apparent height  $\Delta h$ . Reprinted with permission from [58], Copyright 2005, American Institute of Physics.

to various conformations with different heights of a central molecular wire. The Lander molecule (section 2) is a very suitable molecule in this regard. After deposition onto Cu(110) at room temperature, it adsorbs in the parallel legs conformation on a copper nanostructure (figure 4). By STM manipulation at low temperatures of 7 K, it is possible to achieve another conformation, which is not observed directly after adsorption, where the central board is tilted at the end of the contact pad (figure 8). This shows how the vertical distance between the wire and the electrode can be changed in a controlled way. However, the Single Lander molecules exhibit a contact bump only in the tilted board case and none in the other conformations (when the molecule is still completely adsorbed on the nanostructure). It is therefore necessary to take advantage of the Lander characteristics, but to modify the central molecular wire to enhance this effect also in planar configurations of the molecular wire.

The so-called Reactive Lander molecule is almost equivalent to the Single Lander as only a double bond is added to each end group of the molecular wire (figure 14). When these molecules are deposited onto Cu(110), they behave equivalently to the Single Landers as they cause the formation of copper nanostructures under them [33]. Figure 12 shows the manipulation of a single Reactive Lander molecule along such a nanostructure (equivalent to the experiment in figure 8). A comparison of the experimental line scans with calculated ones shows that the molecule adapts to the same conformations as the Single Lander: crossed and parallel legs conformations after a small lateral shift along the nanostructure ((a) and (b)) and the tilted board conformation when the molecule reaches the end of the copper wire (c). The latter one is not planar and therefore shows a larger difference in the intensity of the four lobes corresponding to the four molecular legs. The legs of the Lander molecule are essential in this motion as they keep the central wire always on the nanopad. A further manipulation step results in the complete removal of the molecule from the nanostructure for the case of a Single Lander. However, at this point the Reactive Lander behaves differently as it adapts to another stable conformation, where the four legs are already on the lower terrace, but the end of the molecular board is still in contact with the nanostructure (note that the same conformation can also be achieved by moving the molecule completely on the lower terrace and the pushing it

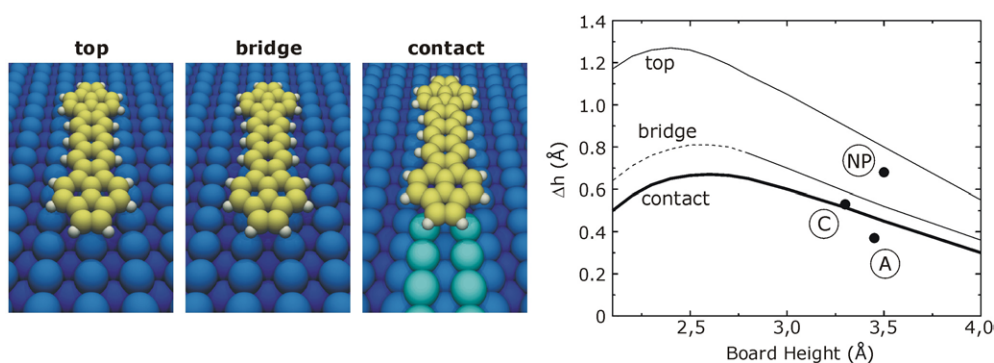


**Figure 13.** Left panel: sphere models of the bare central board (oriented in the  $[1\bar{1}0]$  direction) in top, bridge and contact adsorption positions of the Cu(110) surface. Right panel: STM apparent height  $\Delta h$  at the end board location as a function of the distance of the molecular board from the surface. Solid lines represent calculations whereas circles indicate experimental results for three different conformations (see figure 12): RL in planar contact with the nanopad (C); RL with parallel legs rotated towards the lower terrace (A); RL in the tilted board conformation (NP). At small board heights (below 2.7 Å), the bridge site adsorption curve is estimated (dashed line) as the contact bump from the double bond is overshadowed by contributions from other molecular orbitals. Reprinted with permission from [33]. Copyright 2005 American Chemical Society.

towards the nanostructure). This conformation is called the contact conformation (figure 12(d)), because the double bond at one end of the molecular wire is now interacting with the copper electrode. It imitates very well the ideal case of a contact configuration (figure 1), because the molecular wire, in contact with the nanopad only with its end group, is planar and elevated from the surface. Such a planar contact configuration cannot be obtained with the Single Lander because the board is too short, so the front legs maintain the board end too far away from the end of the Cu nanostructure.

The presence of a contact bump is apparent in the STM images (figures 12(a)–(d)) as an additional intensity at the end of the central molecular board (marked by arrows). Line scans along the  $[1\bar{1}0]$  direction (in (e)) show them more clearly and give quantitative information about their height. These curves confirm the presence of a shoulder, attributed to the interaction between the wire and the metallic electrode, in all cases except the initial conformation one (where the conformation gives no access to the contact position as all legs are rotated towards the upper terrace—see figure 4). This is in contrast to the Single Lander case, where only the tilted board conformation exhibits a contact bump [31]. As can be seen from the line scans, the intensity of this contact bump differs for the observed configurations: for the contact configuration C, a value of  $\Delta h = 0.53 \pm 0.03$  Å is determined, while configuration A shows a  $\Delta h = 0.37 \pm 0.03$  Å. A larger value of  $\Delta h$  is obtained for the non-planar case (configuration NP), where  $\Delta h = 0.68 \pm 0.05$  Å. The crossed legs case can be neglected as it is equivalent to configuration A with one pair of legs rotated. The variation in these intensities is due to the different heights of the central molecular wire above the nanostructure, and thus the interatomic distance between the molecular wire and the contact pad. This distance is known from the calculated molecular conformations: 3.45 Å for conformation A, 3.3 Å for C and 3.5 Å for the tilted board case (NP).

For a better understanding of the contact bump dependence on the vertical distance, it was calculated how the STM contrast produced by the terminal double bond of the RL board alone depends on the distance  $z$  of the board from the Cu(110) surface (no legs were considered). The adsorption configurations studied are shown schematically in the left panel of figure 13.

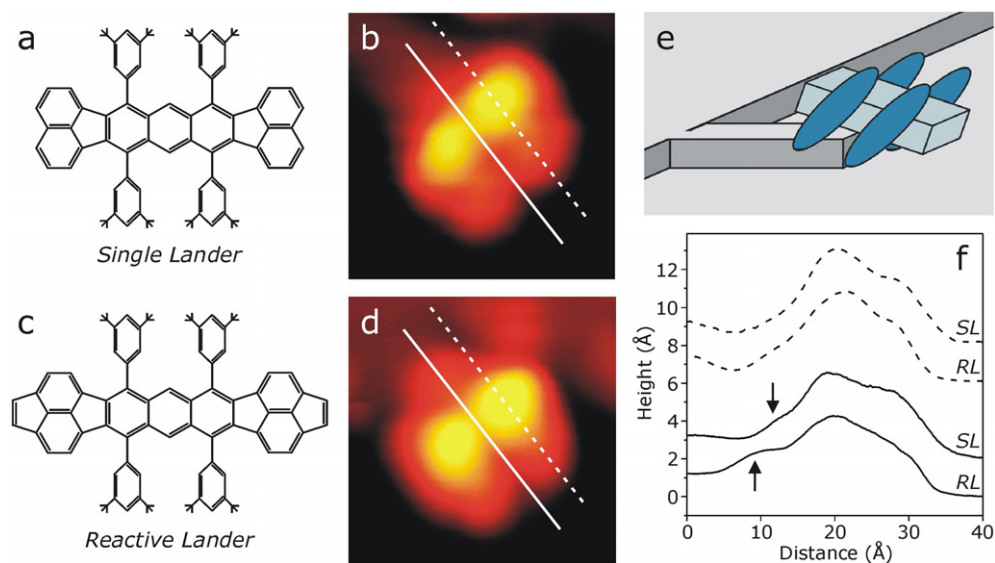


**Figure 14.** Comparison of the electronic contact of the Single Lander (SL; (a)–(b)) [31] and the Reactive Lander (RL; (c)–(d)) [33] molecule in the same conformation. (a) and (c) show the chemical structures, while the corresponding STM images (both  $35 \times 35 \text{ \AA}$ ) of the two molecules are presented in (b) and (d), respectively. Both molecules are in the tilted board conformation, shown schematically in (e). A direct comparison of line scans (taken in the  $[1\bar{1}0]$  direction as indicated in the STM images in (b) and (d)) across the central board (solid line) and the legs (dashed line) of SL and RL molecules in (f) shows a difference of the contact bump intensity (marked by arrows).

The role of the adsorption site of the board was considered by comparing top, bridge and contact adsorptions, where the latter one reflects best the geometry of the experiment. The resulting contact curve in the right panel shows a maximum  $\Delta h$  value for a board height of about  $2.6 \text{ \AA}$  and an approximately linear decrease for higher values, i.e. when the board is lifted up. The experimental data for A and C, plotted in the diagram for the three conformations, are in very good quantitative agreement with the calculations. The relatively large value of the non-planar configuration (NP) is probably due to the electronic interaction not only of the double-bond end but also of the central part of the molecular wire with the end of the nanopad (see the scheme in figure 12(c)). An important result of figure 13 is the *qualitative* agreement between experiment and calculations: in conformation A the electronic interaction between the molecular wire and nanostructure is smaller than in C (both planar contact geometries), because the board height is larger in this case. It is therefore possible to modify the molecular wire height above the electrode and thus the electronic contact in a controlled way by changing the molecular conformation in the experiment.

## 6. Changing the chemistry of the molecular wire's end group

The characteristics of the charge transport through a molecular wire–electrode junction depend strongly on the chemical composition of the wire's end group [21]. Theoretical studies have shown that the enlargement of a benzene to an anthracene group leads to a 20 times larger contact conductance [19]. It is therefore of interest to perform an experiment that compares two cases of very similar molecules, differing only in their end groups. Of course, the electrode and the contact configuration must be equivalent for these two cases in order to exclude other

modifications of the electronic interaction. The molecules of the Lander family are very suitable for such a study, because they differ in the chemical structure of their central molecular board while having the same lateral spacer groups. In particular, the Single and the Reactive Lander offer the ideal conditions for such a comparative study, because they both cause the formation of a copper nanostructure upon the adsorption on Cu(110) [27, 33]. It was shown that they can both be manipulated along this nanostructure, i.e. a contact pad, in a controlled way, adapting to the same characteristic conformations (figures 8 and 12). The tilted board conformation (called also NP), where the molecule has reached the end of the nanostructure in a non-planar configuration, is of particular interest, because it results in the presence of a contact bump at the end of the molecular wire in both cases.

Figure 14 shows a direct comparison of the Single and the Reactive Lander molecules in the tilted board conformation. Their chemical structure differs only in an additional double bond at the terminal groups of the molecular wire with equal lateral 3,5-di-*tert*-butylphenyl legs. Note that the line scans across the molecular legs (dashed curves in (f)) are almost identical for the two molecules, which confirms the adsorption in the same tilted board conformation. This equivalence is not surprising, because the chemical structure of the central board differs, while the conformation is mainly determined by the four legs. Accordingly, their appearances in STM images ((b) and (d)) are very similar, dominated by two intense lobes, which correspond to the two legs closer to the upper terrace. They overshadow the other two legs that appear only as weak shoulders. The height profiles across the molecular board (f) show a contact bump at the end group of the molecular wire for both molecules. Their lateral position is slightly different, reflecting the elongation of the molecular wire. A remarkable difference is present in the intensity of the two contact bumps:  $\Delta h = 0.22 \pm 0.07 \text{ \AA}$  for the Single Lander, but  $\Delta h = 0.68 \pm 0.05 \text{ \AA}$  for the Reactive Lander, which reflects the chemical modification of the end groups of the molecular board.

## 7. Outlook

It was shown how various molecular wires can be placed in contact by STM manipulation, in a controlled way, with metallic electrodes of different shape and dimensions. The result of the electronic interaction achieved between them is an additional contribution to the tunnelling current at the contact position. The next step of the study of electronic contacts should be measurements of transport through the molecular wire. While one electrode could still be a metallic step edge or nanostructure, the second electrode is provided by the STM tip itself, which is positioned at the opposite end of the wire. A planar contact geometry is preferentially maintained, which requires spacer legs attached laterally to the molecular wire, like the Lander molecules. However, the Single and Reactive Landers presented are not suitable for transport measurements as the molecular legs (rotated on purpose towards the lower terrace) do not allow tip access to the end group. Using spacer legs for decoupling of the wire from the metallic substrate, a different approach is therefore necessary, where the molecular wire extends sufficiently from the spacer legs for tip access, but is not yet deformed towards the substrate. Another approach, which avoids the use of spacer legs, is the growth of insulator films on a metal surface. By covering the substrate only partially, a molecular wire could be manipulated onto the border of an insulating region, bridging the gap between metal and insulator (in an ideally planar conformation). This geometry imitates very well the ideal contact conformation if the insulator provides sufficient electronic decoupling.

In a technical application for future molecular electronics, it is fundamental to have many atomic-scale contact pads at one's disposal. The Lander molecules are a good model system in this regard, as they lead to the formation of nanopads by themselves. However, STM

manipulation of each single molecule is required to bring their terminal groups into contact with the electrode. Thus, molecular units must be designed which adsorb directly in a contact configuration, in order to have many molecules available. The other (free) end of the molecular wire should provide the possibility for association of other functionalized molecules. In this way, the molecules could act as contact units for more complex circuits.

## References

- [1] Moore G 1975 *IEDM Tech. Dig.* 11
- [2] Packan P A 1999 *Science* **285** 2079
- [3] Joachim C, Gimzewski J K and Aviram A 2000 *Nature* **408** 541
- [4] Ellenbogen J C and Love J C 2000 *Proc. IEEE* **88** 386
- [5] Heath J R and Ratner M A 2003 *Phys. Today* **56** 43
- [6] Barth J V, Costantini G and Kern K 2005 *Nature* **437** 671
- [7] Aviram A and Ratner M 1974 *Chem. Phys. Lett.* **29** 277
- [8] Dorogi M, Gomez J, Osifchin R, Andres R P and Reifenberger R 1995 *Phys. Rev. B* **52** 9071
- [9] Metzger R M *et al* 1997 *J. Am. Chem. Soc.* **119** 10455
- [10] Zhao J, Zeng C, Cheng X, Wang K, Wang G, Yang J, Hou J G and Zhu Q 2005 *Phys. Rev. Lett.* **95** 045502
- [11] Donhauser Z J *et al* 2001 *Science* **292** 2303
- [12] Ebbesen T W, Lezec H J, Hiura H, Bennett J W, Ghaemi H F and Thio T 1996 *Nature* **382** 54
- [13] Cao J, Wang Q and Dai H 2005 *Nat. Mater.* **4** 745
- [14] Tans S J, Verschueren A R M and Dekker C 1998 *Nature* **393** 49
- [15] Dadosh T, Gordin Y, Krahn R, Khivrich I, Mahalu D, Frydman V, Sperling J, Yacoby A and Bar-Joseph I 2005 *Nature* **436** 677
- [16] Reichert J, Ochs R, Beckmann D, Weber H B, Mayor M and von Löhneysen H 2002 *Phys. Rev. Lett.* **88** 176804
- [17] Kergueris C, Bourgoin J-P, Palacin S, Esteve D, Urbina C, Magoga M and Joachim C 1999 *Phys. Rev. B* **59** 12505
- [18] Strosio J A and Eigler D M 1991 *Science* **254** 1319
- [19] Magoga M and Joachim C 1997 *Phys. Rev. B* **56** 4722
- [20] Lang N D and Avouris P 2001 *Phys. Rev. B* **64** 125323
- [21] Nitzan A and Ratner M A 2003 *Science* **300** 1384
- [22] Kushmerick J G 2005 *Mater. Today* **8** 26
- [23] Gourdon A 1998 *Eur. J. Org. Chem.* **1998** 2797
- [24] Sautet P and Joachim C 1991 *Chem. Phys. Lett.* **185** 23
- [25] Kuntze J, Berndt R, Jiang P, Tang H, Gourdon A and Joachim C 2002 *Phys. Rev. B* **65** 233405
- [26] Langlais V J, Schlittler R R, Tang H, Gourdon A, Joachim C and Gimzewski J K 1999 *Phys. Rev. Lett.* **83** 2809
- [27] Rosei F, Schunack M, Jiang P, Gourdon A, Laegsgaard E, Stensgaard I, Joachim C and Besenbacher F 2002 *Science* **296** 328
- [28] Schunack M, Rosei F, Naitoh Y, Jiang P, Gourdon A, Laegsgaard E, Stensgaard I, Joachim C and Besenbacher F 2002 *J. Chem. Phys.* **117** 6259
- [29] Gross L, Moresco F, Alemani M, Tang H, Gourdon A, Joachim C and Rieder K-H 2003 *Chem. Phys. Lett.* **371** 750
- [30] Moresco F, Gross L, Alemani M, Rieder K-H, Tang H, Gourdon A and Joachim C 2003 *Phys. Rev. Lett.* **91** 036601
- [31] Grill L, Moresco F, Jiang P, Joachim C, Gourdon A and Rieder K-H 2004 *Phys. Rev. B* **69** 035416
- [32] Alemani M, Gross L, Moresco F, Rieder K-H, Wang C, Bouju X, Gourdon A and Joachim C 2005 *Chem. Phys. Lett.* **402** 180
- [33] Grill L, Rieder K-H, Moresco F, Stojkovic S, Gourdon A and Joachim C 2005 *Nano Lett.* **5** 859
- [34] Zambelli T, Tang H, Lagoute J, Gauthier S, Gourdon A and Joachim C 2001 *Chem. Phys. Lett.* **348** 1
- [35] Otero R, Naitoh Y, Rosei F, Jiang P, Thostrup P, Gourdon A, Laegsgaard E, Stensgaard I, Joachim C and Besenbacher F 2004 *Angew. Chem. Int. Edn* **43** 2092
- [36] Otero R, Rosei F, Naitoh Y, Jiang P, Thostrup P, Gourdon A, Laegsgaard E, Stensgaard I, Joachim C and Besenbacher F 2004 *Nano Lett.* **4** 75
- [37] Otero R, Hümmelink F, Sato F, Legoas S B, Thostrup P, Laegsgaard E, Stensgaard I, Galvao D S and Besenbacher F 2004 *Nat. Mater.* **3** 779
- [38] Zambelli T, Jiang P, Lagoute J, Grillo S E, Gauthier S, Gourdon A and Joachim C 2002 *Phys. Rev. B* **66** 075410
- [39] Gross L, Moresco F, Savio L, Gourdon A, Joachim C and Rieder K-H 2004 *Phys. Rev. Lett.* **93** 056103
- [40] Eigler D M and Schweizer E K 1990 *Nature* **344** 524

- 
- [41] Bartels L, Meyer G and Rieder K-H 1997 *Phys. Rev. Lett.* **79** 697
  - [42] Keeling D L, Humphry M J, Moriarty P and Beton P H 2002 *Chem. Phys. Lett.* **366** 300
  - [43] Crommie M F, Lutz C P and Eigler D M 1993 *Science* **262** 218
  - [44] Heinrich A J, Lutz C P, Gupta J A and Eigler D M 2002 *Science* **298** 1381
  - [45] Moresco F 2004 *Phys. Rep.* **399** 175
  - [46] Grill L, Rieder K-H, Moresco F, Jimenez-Bueno G, Wang C, Rapenne G and Joachim C 2005 *Surf. Sci.* **584** L153
  - [47] Moresco F, Meyer G, Rieder K-H, Tang H, Gourdon A and Joachim C 2001 *Phys. Rev. Lett.* **86** 672
  - [48] Lagoute J and Fölsch S 2005 *J. Vac. Sci. Technol. B* **23** 1726
  - [49] Nazin G V, Qiu X H and Ho W 2003 *Science* **302** 77
  - [50] Moresco F, Meyer G, Rieder K-H, Tang H, Gourdon A and Joachim C 2001 *Appl. Phys. Lett.* **78** 306
  - [51] Joachim C, Gimzewski J K, Schlittler R R and Chavy C 1995 *Phys. Rev. Lett.* **74** 2102
  - [52] Nilius N, Wallis T M and Ho W 2002 *Science* **297** 1853
  - [53] Xue Y, Datta S and Ratner M A 2001 *J. Chem. Phys.* **115** 4292
  - [54] Crommie M F, Lutz C P and Eigler D M 1993 *Nature* **363** 524
  - [55] Heller E J, Crommie M F, Lutz C P and Eigler D M 1994 *Nature* **369** 464
  - [56] Stojkovic S, Joachim C, Grill L and Moresco F 2005 *Chem. Phys. Lett.* **408** 134
  - [57] Hallmark V M, Chiang S, Meinhardt K-P and Hafner K 1993 *Phys. Rev. Lett.* **70** 3740
  - [58] Grill L, Moresco F, Jiang P, Stojkovic S, Gourdon A, Joachim C and Rieder K-H 2005 *AIP Conf. Proc.* **786** 490